Bulletin of the Seismological Society of America, 91, 4, pp. 760–780, August 2001

A Reappraisal of the 1894 Atalanti Earthquake Surface Ruptures, Central Greece

by D. Pantosti, P. M. De Martini, D. Papanastassiou, N. Palyvos, F. Lemeille, and G. Stavrakakis

Abstract This article presents the results of new field and aerial photo surveys of the Atalanti fault and of the mesoseismal area of the 20 and 27 April 1894 earthquakes. Coupled with a reanalysis of contemporary reports and previous investigations, these are used to gain a better understanding of the faults responsible for these events and their seismic behavior. The first shock was smaller and probably located inshore or offshore the Malessina peninsula. No resolving field evidence has been found to locate the seismogenic structure responsible for this shock. On the basis of the limited information available, we suggest the Malessina escarpment, a 12-km-long, ENE-trending, NW-dipping fault as a possible structure responsible for this event. On the other hand, the second and largest shock is definitely related to the Atalanti fault *sensu stricto,* a main WNW-trending, N-dipping active fault extending between the Platirema valley (a few km NW of the town of Atalanti) and Larymna. The total length of the rupture recognized in the field is about 32 km, but it can be extended further SE up to 40 km. No evidence for a longer rupture extending some other 20 km to the NW, between the Karagiozis river and Ag. Kostantinos, is found. The complex geometry of the fault with bends and step overs appears to be controlled by preexisting transverse structures. Minimum coseismic vertical throws, measured in the field after more than a century elapsed from the earthquake, are 30–80 cm, thus consistent with contemporary reports indicating 1-m average. Slip rates are not well constrained. The available estimates fall in the range 0.1–0.5 mm/yr confirming the smaller amount of crustal extension taking place in this area with respect to other nearby regions such as the Corinth gulf. No new data are available to define the average recurrence interval typical of the Atalanti fault. However, a reconsideration of the existing information induced us to rule out the possibility that the famous 426 B.C. earthquake occurred on the Atalanti fault. On the basis of the extent and size of the rupture recognized in the field, a M 6.8 is estimated for the second and largest shock.

Introduction

Earthquake geology integrates traditional seismology with geology in the study of large earthquakes. It is based on the observation that large earthquakes produce permanent deformations on the geology and topography of the epicentral area. Distribution, magnitude, and geometry of these deformations are dependent on the location, size, geometry, and kinematics of the seismogenic fault at depth. The description of these types of earthquake effects can also be found in ancient reports describing earthquake damage. At the end of the 1800s, some scientists started documenting these effects in a more systematic way, with the basic understanding that these could provide critical information on the earthquake source. This understanding was clear in G. K. Gilbert's (1884) observations on the great 1872 Owens Valley earthquake. Unfortunately, this approach was not widely followed and, even nowadays, there are several earthquakes for which geological observations are not enough taken in consideration.

The careful and objective reporting of features such as major and minor ground ruptures, tilt of strata and surfaces, drainage diversions, coastal uplift and subsidence, and liquefaction, tsunamis, and land-sliding induced by recent large earthquakes is a precious reference and calibration for the study of the earthquakes of the past (paleoearthquakes) for which limited or no historical information are available. For these earthquakes knowledge can only be sought through geological and geomorphic investigations.

The 1894 Atalanti earthquake in central Greece is one of the best documented historical events of surface faulting in the Mediterranean area. Even so, many important aspects of this earthquake are still poorly understood. A better comprehension of these aspects would be very important for the assessment of the seismic hazard of the region because it would contribute to the definition of the 1894 earthquake source and at the same time to the understanding of the neighboring seismogenic structures threatening the area. This is why, after more than a century, we have reappraised the 1894 earthquake, using contemporary reports (Davison, 1894; Mitsopoulos, 1894, 1895; Papavassiliou, 1894a,b; Philippson, 1894; Skouphos, 1894) coupled with investigations performed in the 1970s by Lemeille (1977) and a new aerial photo and field survey. Even though Lemeille's observations were made 80 years after the event, we found them very useful because they were based on new concepts and experience developed in the time elapsed since the earthquake. Lemeille's observations also predate the strong and fast human modification started with the systematic employment of bulldozers in agricultural activities.

Our task is to use the subtle field evidence of the ruptures that remains since the time of the earthquake to better characterize the fault and understand the 1894 earthquake and the seismogenic structure responsible for it.

The Atalanti Fault and the 1894 Earthquakes

Central Greece is a region well known for its active and fast extension. This regime is depicted vividly in the presence of a series of subparallel graben oriented roughly WNW–ESE: the gulf of Corinth, which is the most active of all, the basin between Mt. Kallidromon and Mt. Parnassos, the Lokris (Renghinion) basin, and the North Evoikos gulf (Fig. 1B). The overall motion across Central Greece is NE–SW, with roughly equal amounts of N–S extension and E–W dextral shear, the latter being caused by the motion of the Anatolian plate relative to Eurasia, along the North Anatolian fault zone (e.g., Roberts and Jackson, 1991; Armijo *et al.,* 1996) (Fig. 1A).

The Atalanti fault, striking N110–120° and accommodating prevalently normal movement, is one of the major structures on the SSW side of the N. Evoikos graben, which, according to Philip (1974), is subsiding at a rate of about 1 mm/yr. The fault trace can be well recognized in the geomorphology between the towns of Atalanti and Larymna (Fig. 1C). The topographic contrast between footwall and hanging wall is highest to the NW, in the Rhoda mountains (Chlomon range) near the town of Atalanti where it reaches about 800 m, to decrease to the SE to 500 m and 200 m (Fig. 1C). This important decrease may suggest a substantial change in the rate of slip along the fault, as already proposed by Ganas (1997) and Ganas *et al.* (1998) on the basis of the estimated total displacements across the fault, or it may be related to preexisting topography inherited from previous tectonic activity (i.e., the main peaks of Chlomon range could already have been a regional high when the Atalanti fault started to be active).

The Lokris region was struck by two large shocks that occurred a week apart, on 20 April and 27 April 1894, and were followed by numerous aftershocks. There is substantial agreement in recognizing the Atalanti fault as being responsible for these events. According to contemporaneous reports and recent reanalyses, the first shock was smaller. Ambraseys and Jackson (1990) estimated an equivalent magnitude calculated from felt reports (M_e) of 6.4 and 6.9 for the first and second shock, respectively; whereas higher estimates of 6.7 and 7.0, and 6.7 and 7.2, have been proposed by Makropoulos and Kouskouna (1994) and by Papazachos and Papazachou (1997), respectively. The same authors essentially agree on the macroseismic location of the second and largest shock a few kilometers NE of Atalanti, whereas less agreement exists on the location of the first shock (Fig. 2). A substantially different location for the second shock, about 10 km to the NE of Atalanti (Fig. 2), has been proposed by Karnik (1971).

Damage from the first shock is reported between Arkitsa and Larymna, whereas damage from the second extends from Larymna as far as to Ag. Kostantinos to the north (Fig. 2). The overlap of damage produced by these events makes it hard to discriminate the events. However, it is clear from the damage distribution provided by Ambraseys and Jackson (1990) that the mesoseismal area for the 27 April shock completely contains that of the 20 April shock (Fig. 2).

Ground ruptures, landslides, and major disturbances of the landscape are described by contemporary authors with general consensus about their location and size (Fig. 2) but with very different interpretations about their meaning. The main issue was the extent of the main rupture, called the "great chasm of Lokris," and whether it was a structure continuing at depth (tectonic) or a superficial gravitational feature. Advocates of the first opinion were Skouphos (1894) and Papavassiliou (1894a,b) (joined by A. Philippson [1894] who probably did not make field investigations himself, however), with Mitsopoulos (1895) on the opposite side. Skouphos' published account of the ground effects is the richest in observations, and his writings are referenced frequently in this article.

The first shock appears to have produced small ruptures, cracks, and landslides mainly in the Malessina peninsula and along the coast (i.e., mostly liquefaction effects). These effects were described by Skouphos (1984) as being secondary with respect to those produced by the second shock that seriously perturbed the whole area between the town of Ag. Kostantinos and Cape Gatza. Most ruptures from the second shock appear systematically arranged along or very close to the Atalanti fault with exceptions such as the liquefaction effects along the coastal area, the landslide in Skender-aga (now Megaplatanos), and some poorly described ruptures, such as the Moulkia rupture and the discontinuous ruptures between Atalanti and Ag. Kostantinos. In summary, Skouphos describes a 60-km-long fracture with vertical throws

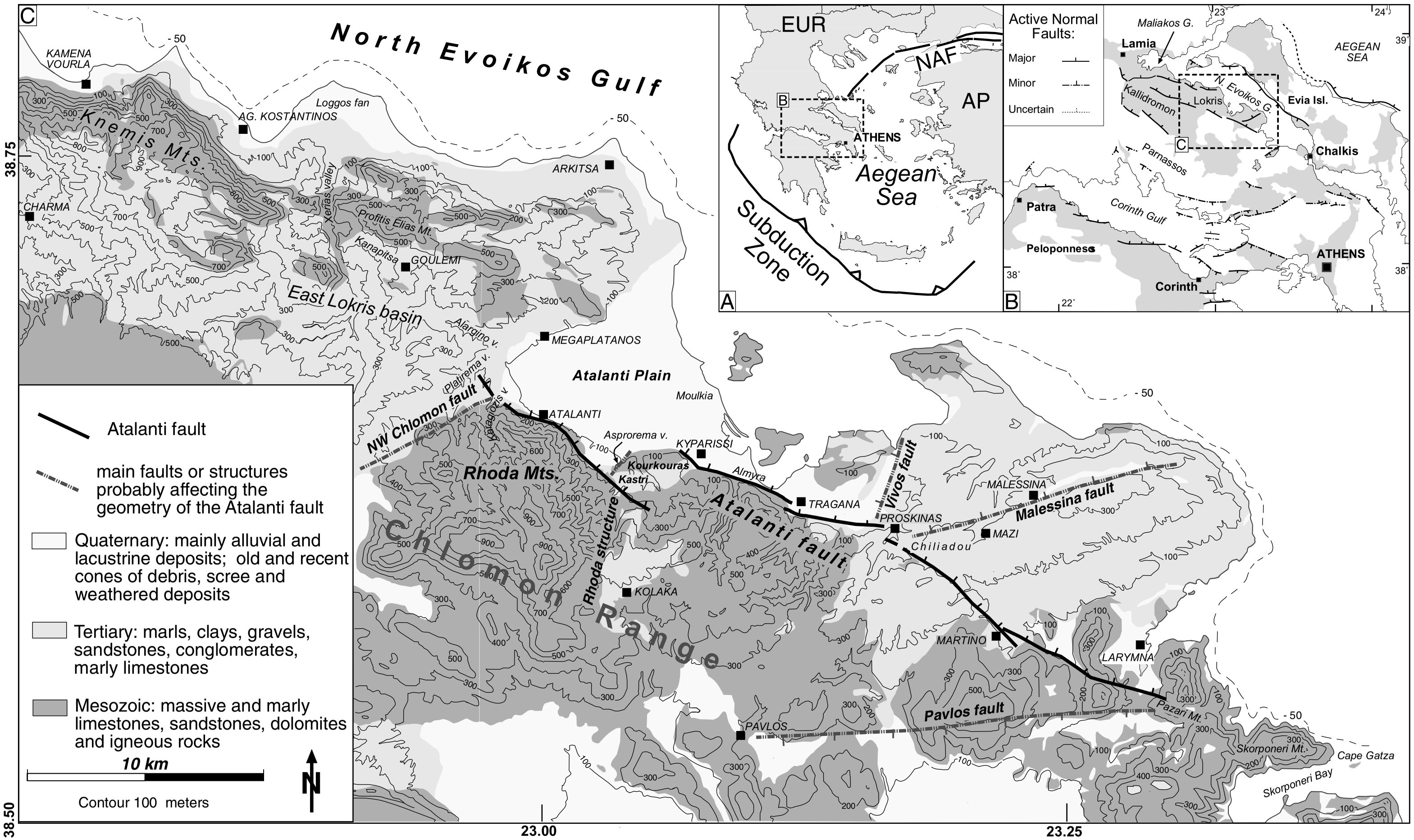

Figure 1. (A) Simplified geodynamic setting of the Aegean region; AP, Anatolian Plate; EUR, Eurasian Plate; NAF, North Anatolian fault zone. (B) Active faults in central Greece, modified from Roberts and Jackson (1991) and Armijo *et al.* (1996). (C) Simplified geology and topography of the area between Ag. Kostantinos and Cape Gatza. The Atalanti fault is mapped along with some other secondary but morphologically visible faults and the Rhoda structure. These faults/structures seem to have an important control on the geometry of the Atalanti fault. The localities mentioned in the text are reported.

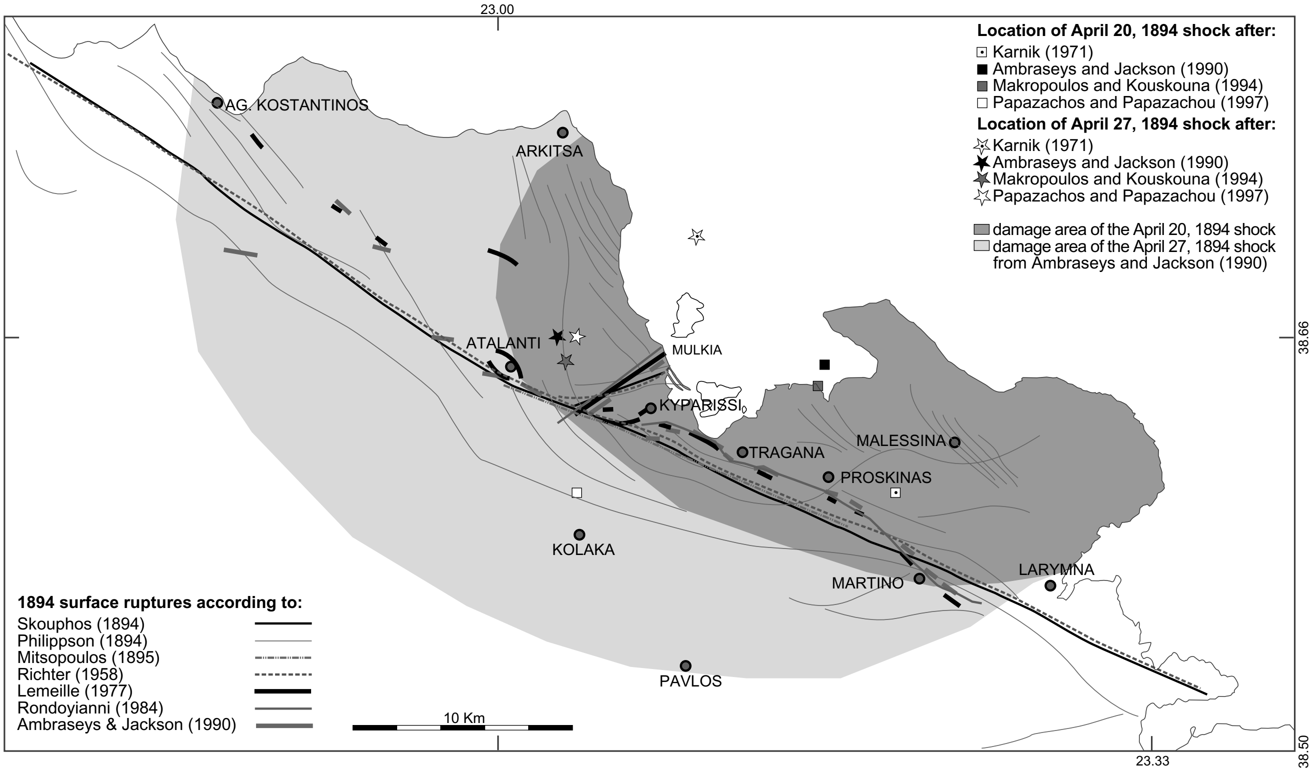

Figure 2. Summary of information available for the 1894 events in published literature. Damage areas, macroseismic and instrumental locations, and traces of surface ruptures are reported. Notice that there is a certain consistency among the traces especially considering the limited availability of detailed maps at the time of the earthquake. Clear exception is the Philippson (1894) thick net of ruptures that probably overestimated the size and extent of cracks and also included pure liquefaction effects. As Philippson himself wrote, he based his Short Note on the reports of Skouphos, Mitsopoulos, and Papavassiliou, plus a map published in the newspaper *Estia.* We examined the original map (*Estia,* n. 48, 23 April 1894), but there is no indication in the figure caption of who plotted the ruptures.

NE side down that range from 30 cm (down to 5–6 cm) in the limestone (i.e., along the bedrock faults) to greater than 1 m (up to 2 m) in alluvium, with variable openings and some undefined left-lateral component. A similar figure is provided by Papavassiliou (1894a,b) although with less details; whereas a much shorter rupture, at the contact between bedrock and alluvium between Halmyra and the Karagiozis river is proposed by Mitsopoulos (1895) (Fig. 2).

The first author reanalyzing these reports was Richter (1958). He concluded that the earthquake produced a 55-km-long rupture and highlighted a left-lateral component of movement. Through a careful investigation with the local population that eye-witnessed the earthquake, or, more commonly, that knew about it through family narrative, Lemeille (1977) made a field reconstruction of the major earthquake effects that is essentially in agreement to those mapped by Skouphos (1894) (Fig. 2). Nowadays several of these ruptures, which in the 1970s appeared still fresh, have been bulldozed and retreated. Thus, they disappeared or can be recognized only as gentle and wide scarps in the agricultural fields. Because of this and also following the scientific trend of the time, most attention in recent years was devoted to bedrock fault scarps that are the most obvious and clearly the most resistant to both human and natural erosion. After the work of Lemeille (1977), the Atalanti fault was the object of several studies. Rondoyianni (1984) studied the fault within the neotectonic framework of the area. Stiros and Rondoyianni (1984) investigated possible aseismic movements along the fault through geodetic leveling and concluded that they are up to 1 mm/yr. Ambraseys and Jackson (1990) presented a map of the 1894 ruptures and the damage distribution for both shocks. Collier and Gawthorpe (1994) proposed a segmentation model based on drainage patterns. Poulimenos and Doutsos (1996) suggested the existence of barriers that possibly control the rupture propagation and proposed a model to predict the future evolution of the fault. Ganas (1997) and Ganas *et al.* (1998) (1) defined the segment boundaries of the fault just NW of Atalanti and near Larymna through structural observations and geomorphic interpretation of Landsat images (Fig. 2), (2) estimated maximum slip rates for the fault of 0.27–0.4 mm/yr on the basis of throw profiles on Neogene or pre-Neogene deposits, (3) concluded that the 1894 rupture does not appear to have violated the segment boundaries as inferred, and (4) considered the famous 426 B.C. earthquake (see, for e.g., Papazachos and Papazachou, 1997) as the most probable pre-1894 earthquake on the Atalanti fault. Ganas and Buck (1998) compared a multilayer dislocation model proposed by Ma and Kusznir (1995) for a ~48-km-long, 55°-dipping fault with ~1 m slip, with the subsidence recorded at the archaeological site of Halae (Theologos), to reconstruct the change of shoreline due to tectonic movements in historical time. Cundy *et al.* (2000) studied the coseismically subsided coastal deposits and compared the amount of subsidence they estimate to that predicted by standard dislocation modeling by Ward and Valensise (1989). The authors conclude that the assumption of a coseismic movement of 1 m is reasonable for the 1894 earthquake.

Very limited work has been done to understand the seismic behavior of the Atalanti fault (i.e., estimate of slip per event, repeat time, rupture length, etc.). Makropoulos and Kouskouna (1994), reevaluating the intensities of the 1894 earthquakes, conclude that no earthquakes of a such large intensity are known to have occurred in the same epicentral area in historical time; thus, they rule out the possibility that the 426 B.C. earthquake could be an ancestor of the 1894 event. As mentioned previously, this was instead the hypothesis of Stiros and Pirazzoli (1995), Ganas (1997), and Ganas *et al.* (1998). The latter use the time elapsed between 426 B.C. and 1894 to support a recurrence time of 2500 yr for the Atalanti fault, which they derived from slip rate and coseismic slip.

A Reanalysis of the 1894 Rupture

A recent field and aerial photo survey along with Lemeille's (1977) observations and contemporary reports enabled us to reanalyze the 1894 earthquake rupture. As already mentioned, the contemporary authors, and particularly Skouphos, defined the ground effects produced by the 20 April shock as very secondary with respect to those produced by the 27 April shock. The April 20 ruptures appear concentrated in the Malessina peninsula, and only some small cracks appeared on the roads around Martino, generally at the contact between bridges and artificial embankments. The problem in reinterpreting Skouphos (1894) report is that, with exception of the introduction to his chapter VI, he never discusses the temporal evolution of the ruptures again. Thus, some uncertainty remains. To proceed in our reanalysis, without temporal biases we divide the epicentral zone in three regions: (1) Malessina peninsula and the eastern section of the Atalanti fault, from Cape Gatza to Proskinas; (2) the central and western section of the Atalanti fault, from Proskinas to Atalanti; and (3) the western part of the mesoseismal area in the Lokris (Renginion) basin, from Atalanti to Ag. Kostantinos (Figs. 1 and 3). Tables 1–3 contain more information on sites and areas described in the following text; sites location are shown in Figure 3.

Malessina Peninsula and Eastern Atalanti Fault, from Cape Gatza to Proskinas

According to Skouphos (1894), two sets of ruptures occurred in this area: those in the Malessina peninsula and those along the Atalanti fault *sensu stricto.*

Malessina Peninsula Ruptures. Most of the ruptures described in the contemporary reports occurred in the Malessina valley, near the towns of Mazi and Malessina (sites 1 and 2 in Table 1). None of these ruptures was found during our recent field survey; only gentle breaks in slope at some locations along the SE side of the abandoned Malessina valley and some wide benches along the few active fans draping it have been recognized. Whether these features are related to the present tectonic activity, remnants of previous Quaternary tectonic events, or evidence of large mass movement remains unsolved. The fact that the underlying lithologies (Neogene) are relatively soft may be the reason for the poor preservation of possible 1894 features and previous ones.

However, the 1894 ruptures appear to be located in and aligned with the Malessina escarpment, the principal ENE-trending lineament in the peninsula (Fig. 1C). This escarpment is a structure clearly discernible in satellite images, aerial photos, topographical maps, and in the field. A large normal fault striking 240° is exposed along the cut of the new National Road (close to site 8 in Fig. 3). This structure displaces and downwarps Neogene deposits (north side down) and is part of the Malesina zone of deformation. The whole Malesina structure has a length of about 12 km and appears to produce subsidence to the NW and to be responsible for the general tilt of the Neogene deposits to the SSE. This tectonic setting is exhibited by the geomorphology, drainage patterns, and the location of one of the few areas of recent deposition in the peninsula and would suggest that the Malessina escarpment is presently active. This, along with the location of the 1894 ruptures, suggests a possible involvement of the Malessina structure in the 20 April shock.

Eastern Atalanti Fault Ruptures between Cape Gatza and Proskinas. The second set of ruptures occurred along the main trace of the Atalanti fault; although more important than those produced by the first shock, these ruptures are defined by Skouphos as minor with respect to those observed near the town of Atalanti. He traces the main fault as starting from Cape Gatza, cutting the southwestern slope of Mt. Skorponeri, and the corresponding slope of Mt. Pasari, to continue to Martino and Chiliadou (Fig. 1C).

The 1894 ruptures as described by Skouphos have been recognized at different sites by Lemeille (1977), Ganas (1997), and during our survey (sites 3 to 11 in Table 1 and Fig. 3). Although important modification occurred in the area, small free faces or gentle warps in the agricultural fields are still visible, and we interpret them as evidence for the 1894 coseismic ruptures (Figs. 4 and 5). These ruptures are part of or are parallel to a major cumulative scarp that is the long-term morphological expression of repeated activity

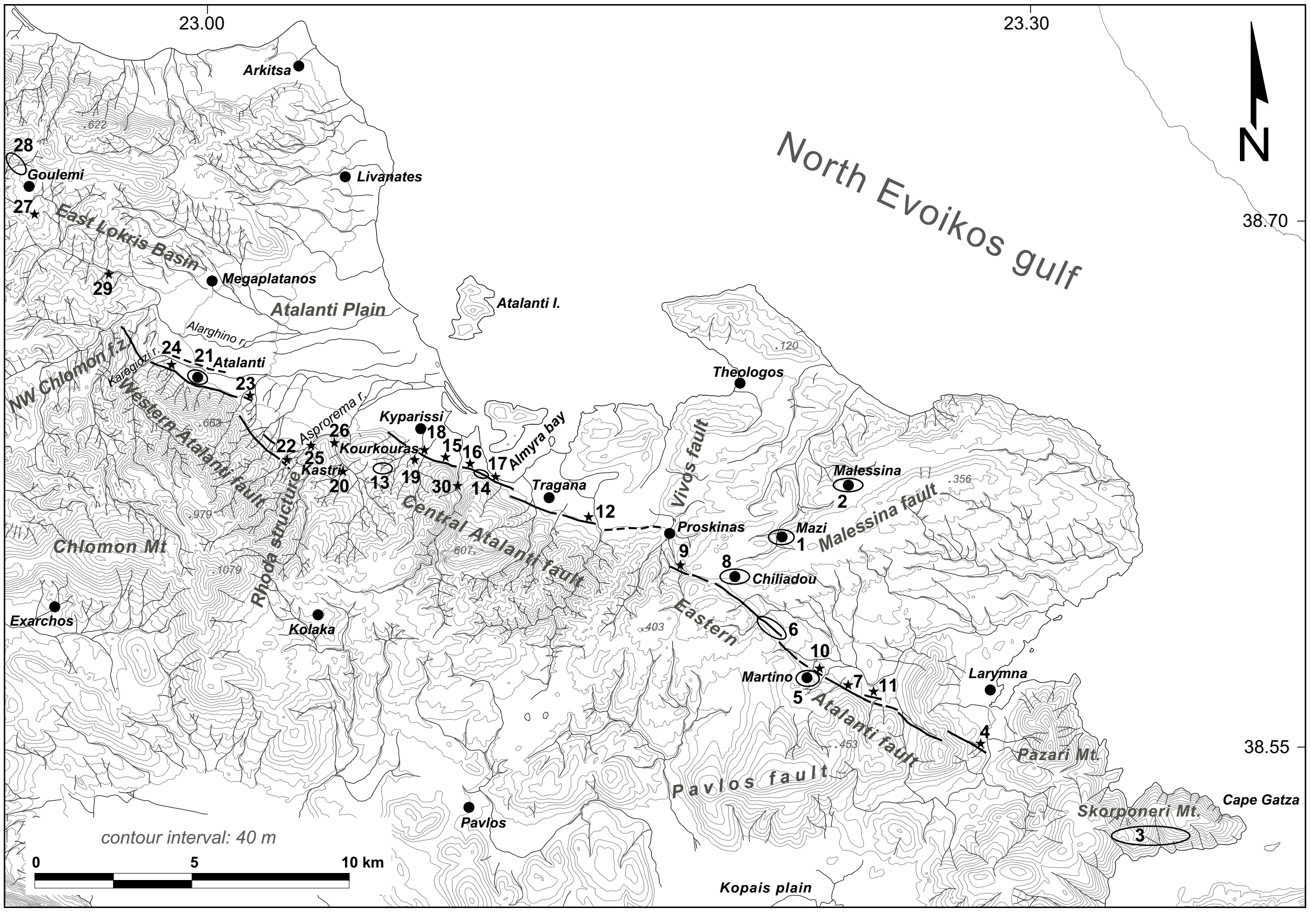

Figure 3. Topographic map of the Atalanti fault region with isolines traced each 40 m. Surface ruptures produced by the 1894 earthquake along with evidence for cumulated ruptures of that and previous events are reported with the thick line. Stars/ellipses with numbers indicate locations/areas described in the text.

along the Atalanti fault. This is very clear in the Neogene deposits between Chiliadou and Larymna where a typical normal faulting escarpment with an average strike NW–SE interrupts the plateau where the town of Martino is built. Double crests, small saddles, and fault bounded basins occur in the promontory between Larymna and Martino. At some locations, fault planes are found in bedrock. Moving away from this well-defined sector, morphology changes significantly. To the west, between Chiliadou and Proskinas, where the Atalanti fault intersects the Malessina and Vivos structures (Ganas, 1997; Ganas *et al.,* 1998), it cannot be traced unequivocally and appears to bend to a more westerly direction. Similarly, to the east of site 4 (Fig. 3), at its intersection with the Pavlos fault, the Atalanti fault cannot be traced further because there is no morphological expression or evidence from the aerial photo and field survey. Conversely, on the basis of satellite imagery analysis, Ganas *et al.* (1998) trace the fault also between Larymna and Cape Gatza. Southeast of Larymna, the deformation appears distributed on several secondary faults (Lemeille, 1977), some of which are obvious in the bedrock, and are possibly related to previous tectonic activity. The lack of clear long-term evidence for the fault between Larymna and Cape Gatza make it hard to understand whether the ruptures described by Skouphos occurred because of direct reactivation of some of the secondary splays, sympathetic slip, or gravitational movement.

The Atalanti Fault, from Proskinas to Atalanti

According to the contemporary authors, this is the part of the fault where the 1894 ruptures were the most impressive and continuous and formed unambiguously during the second shock. The ground ruptures can be divided in three main groups (Fig. 3): the ruptures along the Atalanti fault between Proskinas and Kyparissi, those between Asprorema and Karagiozis rivers, and the ruptures along a transversal lineament following the Asprorema valley (NE–SW Moulkia ruptures).

The Central Section of the Fault between Proskinas and Kyparissi. No detailed contemporary description of the

Table 1
1894 Earthquake Ruptures in the Malessina Peninsula and along the Eastern Atalanti Fault*

Site		Description
1 MP	S	Near Mazi, NE–SW ruptures produced sliding of some orchards (1 m vertical and 12(?) m horizontal, possible landslide?). Other NE–SW ruptures with maximum length of 150 m.
	O	Not mentioned.
	W	Not found.
2 MP	S	Near Malessina, new NE–SW ruptures formed where old faults already produced a staircase conformation of the ground. They did not exceed 200 m in length and cut the market place.
	O	Not mentioned.
	W	Wide benches and gentle breaks in slope possibly related to Skouphos description.
3 SA	S	Rock and cave falls. Ruptures southeast of Larymna, as far as Cape Gatza.
	O	Lemeille (1977): no evidence found possibly because ruptures are distributed in a wide area.
	W	Not found.
4 EAF	S	Major open ruptures more than 200 m long in cemented conglomerates, with reddish water flowing out of them near Larymna. Scarps up to 30 cm high in limestone and larger ruptures in the Neogene and alluvial deposits.
	O	Ganas (1997) describes this location (photo 5.16).
	W	About 1 km south of Larymna, a scarp in bedrock is visible along with open cracks and steps in slope deposits that may represent the degraded 1894 ruptures.
5 EAF	S	In Martino the rupture disrupted the town fountain and produced also some disturbances in the local hydrological setting.
	O	Not found.
	W	Not found.
6 EAF	S	To the NW of Martino the rupture crossed the road to Proskinas.
	O	Not mentioned.
	W	Faults in bedrock.
7 EAF	S	Not specifically mentioned.
	O	Lemeille (1977): 25-cm-high fresh scarp in bedrock at the base of a ~1-m-high degraded bedrock scarp east of the town of Martino (Fig. 5). Ganas (1997) found this rupture and also another in a site nearby; he concludes that this is the only preserved of the 1894 coseismic ruptures.
	W	Intense human modification allows only clear recognition of the main cumulative bedrock scarp.
8 EAF	S	Not specifically mentioned.
	O	Lemeille (1977): Fresh open fractures in limestone bedrock near Chiliadou.
	W	Not found.
9 EAF	S	Not specifically mentioned.
	O	Lemeille (1977): 30- to 50-cm-high scarplet crossing the Krya Vryssi stream.
	W	Subtle scarp in slope deposits.
10 EAF	S	Not specifically mentioned.
	O	Not specifically mentioned.
	W	Below the town of Martino in the olive fields: gentle warp of the surface, up to 3 m-high, about 1000 m long (Fig. 4). Scarp located a few tens of meters north of the main escarpment; interpreted as cumulative scarp. Hidden and protected by bushes and brambles, remnants of the 1894 rupture in slope deposits with visible free faces 20–30 cm high are found.
11 EAF	S	Not specifically mentioned.
	O	Not specifically mentioned.
	W	East of Martino: remnants of a cumulative scarp parallel to the main basin bounding morphological escarpment may contain the 1894 rupture. Intense agricultural modification.

*Location of sites shown in Figure 3. MP, Malesina Peninsula; SA, Skorponeri area; EAF, East Atalanti fault; S, from Skouphos (1894); O, from other works; W, this article.

ruptures between Proskinas and Tragana was found. Lemeille's and our recent survey revealed the existence of fresh scarplets in bedrock and of a cumulative scarp that generally appears as a gentle warp when on recent slope deposits (site 12 in Table 2).

Between Tragana and Kyparissi the ruptures should have been impressive and with a quite simple and linear geometry. The only significant complexity mentioned by Skouphos is a bifurcation of the ruptures SW of Kyparissi (site 13 in Table 2). Skouphos describes scarps up to 30 cm high in limestone (see for example plate XV in Skouphos, [1894]) and larger ruptures in Neogene and alluvial deposits that according to our survey and interpretation should have been generally parallel to each other; thus, they were splays at the surface of the same fault plane at depth.

Although modified by construction of the national road and agricultural works, the 1894 rupture can be well recognized at the bottom of the mountain slope all along the

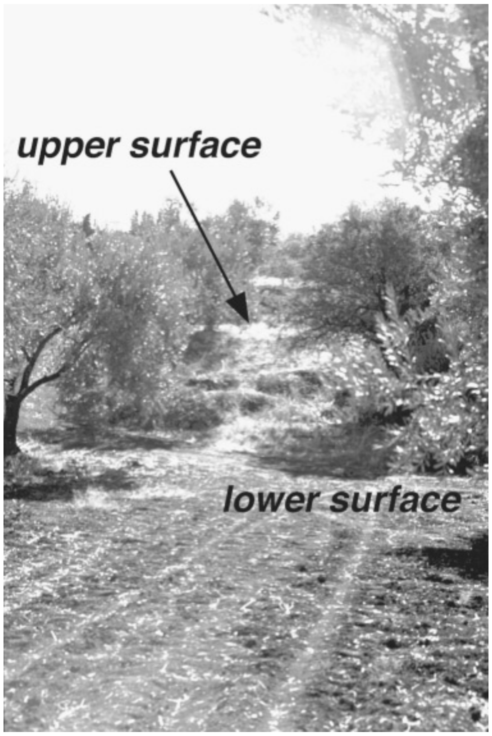

Figure 4. View from NE of the cumulative scarp near Martino (site 10 in Fig. 3). Although there is substantial human modification, a ~3-m-high scarp affecting colluvial and alluvial surface can be measured. Locally remnants of possible 1894 free-face are found.

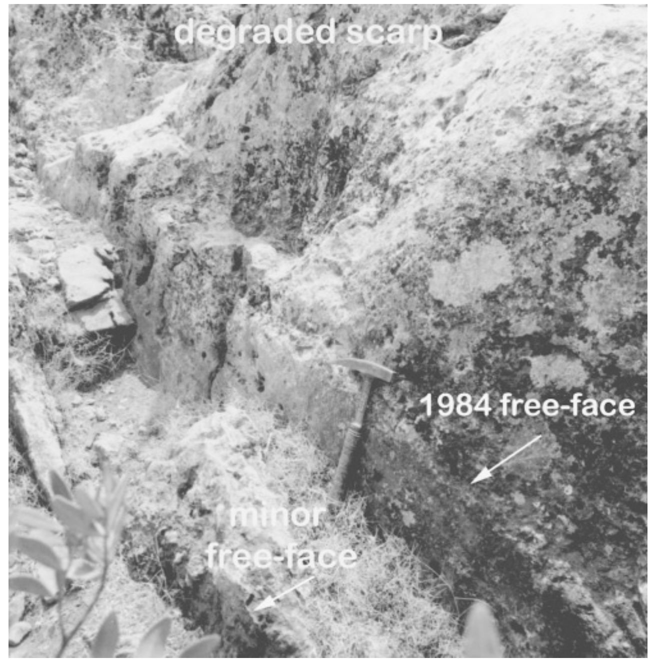

Figure 5. Detail of the 1894 fault scarp in bedrock at site 7 of Figure 3, east of Martino. This photo was taken in the 1970s, about 80 years after the earthquake. Notice the double rupture at the surface. Photo courtesy of J. Tchalenko.

section Tragana–Kyparissi (sites 14 to 18 in Table 2). Close to Tragana these ruptures appear as polished fault surfaces in the limestone and crop out at the base of degraded fault planes; to the west near Almyra and Kyparissi some discontinuous scarplets can be recognized in the bedrock as well as degraded scarps in slope wash and alluvial deposits (Figs. 6 and 7). Unfortunately, nowadays the scarps in soft sediments are often retreated artificially to set or to enlarge olive groves. However, if bulldozing was not totally disruptive it is still possible to obtain a rough estimate of the 1894 displacement of the original surface by using topographic profiles (e.g., Fig. 8A).

The ruptures in the area between Kyparissi and Proskinas run very close to and fit well the long-term geomorphic expression of the Atalanti fault. This is a typical normal fault range front, quite rectilinear with a few large triangular facets and a few wine-glass valleys; only small stepovers interrupt its continuity. West of Proskinas the fault is about E–W to reach 290° near Tragana. The range front shows ~0.5 km right step W of Tragana and becomes a very steep, rectilinear front, up to 500 m high. This section of the fault strikes consistently 290–295° and shows an increase of steepness at the base of the slope. South of the village of Kyparissi, the fault probably crosses the valley to join the northern front of Kourkouras hill where a few small fault planes in bedrock crop out. Thus, evidence for the fault becomes unclear probably because it dies out upon entrance in the Atalanti alluvial plain. Some authors suggest that the fault does not die out, but from that point on it makes a sharp bend toward SW following the Asprorema river (see following discussion for this aspect).

The Western Part of the Fault between Asprorema and Karagiozis. According to Skouphos (1894), these ruptures bounded the northern slopes of the Rhoda Mountains and continued through Atalanti to as far as the Karagiozis river (Figs. 1C and 3). Skouphos was particularly focused on the complexity of the ruptures observed in the town of Atalanti where a secondary splay diverted from the main trace SE of the town to surround it and to join again the main rupture to the west (site 21 in Table 3). It is not completely clear from the Skouphos report whether this secondary splay had an antithetic or synthetic geometry. The topography and the drainage pattern of the Atalanti town area are suggestive of an antithetic secondary fault delimiting a small graben.

Several locations with evidence for the 1894 ruptures have been found during our survey. Most of them are part of a continuous ground flexure parallel to the range front (sites 23 and 24 in Table 3, Fig. 9). This feature is also visible in the 1985 aerial photos despite the intense agricultural activity on the fans draping the southern part of the Atalanti plain. Possible 1894 free faces have been recognized at sites 21 and 22 (Table 3).

Table 2
1894 Earthquake Ruptures along the Central Section of the Atalanti Fault*

Site		Description
12	S	Not specifically mentioned.
	O	Lemeille (1977): 30- to 60-cm-high scarplets within the morphologic scarp in bedrock and colluvium near Agios Dimitros, (see for example plate V in Lemeille (1977); not visible today because of intense agricultural works).
	W	3-m-high wide flexure of the ground surface is accompanied by a clear back tilt of the hanging wall; it is parallel to the morphologic escarpment that is located about 100 m to the south. The intense bulldozing for agricultural purposes makes it hard to recognize this feature. We interpret this flexure as the cumulative evidence of repeated ruptures, the most recent of which would be that of 1894. Total vertical coseismic throw in this area should be derived from the summation of the throws in the bedrock and in the slope wash, which amounts to more than 30–60 cm.
13	S	SW of Kyparissi: 2-km-long, 800-m-wide NW-elongated, elliptical-shaped rupture encircling, a Tertiary hill, 35- to 40-cm subsidence and 25- to 45-cm opening. Bifurcation of the main fault.
	O	Lemeille (1977): evidence of the ruptures not found. Bifurcation tentatively mapped at the contact between Neogene deposits and Mesozoic limestone (Fig. 2).
	W	No conclusive evidence for the rupture bifurcating near Kyparissi have been found. Information from a local person recalling in his childhood evidence for the 1894 rupture following a curved route starting in the vicinity of Ag. Panteleimonas (site 20) and continuing toward Ag. Ioannis site 18 (hearsay?). Geomorphic indications for possible movement along old faults at the contact between soft (Neogene) and compact (Mesozoic) deposits (subsidence to the south). Possible surface effects due to seismic waves propagation.
14	S	Occurrence of important rock falls all along the mountain front in Almyra.
	O	Mitsopoulos (1895): fallen limestone boulders appeared at night as pasturing sheep.
	W	Huge fallen blocks still visible, see Figure 7A.
15	S	Scarps up to 30 cm high in limestone and larger ruptures in the Neogene and alluvial deposits.
	O	Lemeille (1977): 60-cm-high scarp on slope deposits (Fig. 6).
	W	Highly modified scarp (olive grove boundary).
16	S	Scarps up to 30 cm high in limestone and larger ruptures in the Neogene and alluvial deposits.
	O	Not specifically mentioned.
	W	Scarp in slope deposits, 80-cm minimum coseismic throw (Fig. 8A). Trenching in nearby site where scarp is still preserved (Fig. 7) shows very complex rupture with several splays; total vertical 1894 movement of ~60 cm (Pantosti *et al.,* 2000).
17	S	Scarps up to 30 cm high in limestone and larger ruptures in the Neogene and alluvial deposits.
	O	Ganas *et al.* (1998) upon lain Stewart indication; ~53 cm coseismic footwall uplift from a fresh water notch, indented in the limestone footwall of the fault at the Tragana spring, that appears uplifted relative to the present spring water level.
	W	About 50-cm 1894 footwall uplift from the spring notches considering that spring level is directly controlled by the sea level (very close to the shoreline with salt mash in front of it) and prior to the earthquake it was probably the same. Recent landfills (winter 1999) for the widening of the national highway have buried the spring mouth.
18	S	Not specifically mentioned.
	O	Lemeille (1977): scarp in alluvium indicated by local people.
	W	Degraded cumulative scarp in agriculture fields on the NW prolongation of the scarp of site 15. Well preserved scarp at the base of a small church (Ag. Ioannis).
19	S	Not specifically mentioned (the archeological remains were buried at the time of the 1894 earthquake).
	O	Stiros (1988) and Stiros and Pirazzoli (1995): displacement (faulting) of the foundations of an ancient *stoa* (Greek building) located close or on the fault. Abandonment of *stoa* dated to 450 B.C. interpreted as due to an earthquake.
	W	Possibly of landsliding suggested by topography. Age of abandonment poorly constrained. Possible displacement/landsliding in 1894 as suggested from the change in slope shown in Stiros (1988) representation of the site.
20	S	Not specifically mentioned.
	O	Not specifically mentioned.
	W	Ag. Pantelelmonas: Information from a local person recalling in his childhood evidence for the 1894 rupture following a curved route starting here and continuing towards Ag. Ioannis site 18 (hearsay?). This may represent the bifurcation described by Skouphos and thus a possible continuity or a linking structure between the Karaglozis–Asprorema ruptures and those of Kyparissi–Proskinas east of Kourkouras hills.

*Location of sites in Figure 3. S, from Skouphos (1894); O, from other works; W, this article.

Evidence of long-term activity of the Atalanti fault between Asprorema and Karagiozis river is very obvious although most of the 1894 ruptures we found are located off but parallel to the main tectonic escarpment formed by volcano-sedimentary Triassic rocks raising up from the alluvial fans. This suggests a complexity of the 1894 rupture that appears distributed over a wide zone of deformation between the bedrock escarpment and the wide flexure. The northern range front of the Rhoda Mountains appears as a typical active normal fault front with high linearity charac-

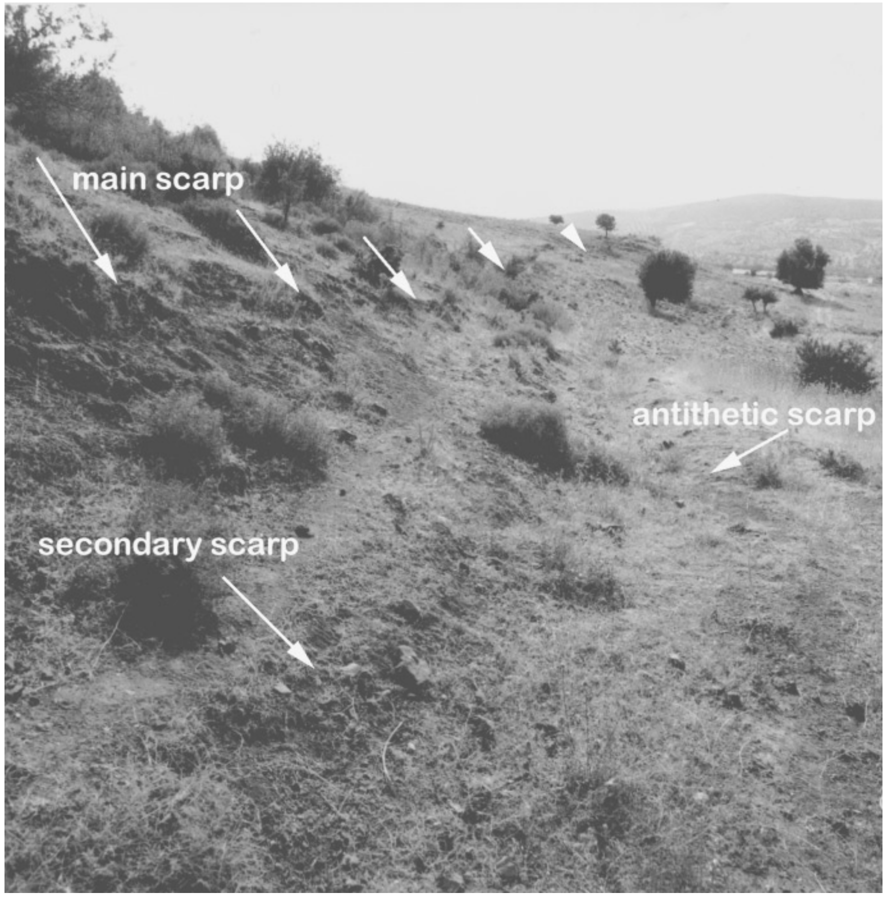

Figure 6. View of the 1894 fault scarp at site 15 of Figure 3, SE of Kiparissi. This photo was taken in the 1970s, about 80 years after the earthquake. Notice the complexity of the rupture that appears composed by several subparallel scarps, clearly visible are at least two main synthetic and one antithetic scarps. This complexity has been also observed at other sites and in the trenches, Pantosti *et al.* (2000). Photo courtesy of J. Tchalenko.

terized by triangular facets (Fig. 10), wine-glass valleys, and increased steepness at the base (Ganas and White, 1996; Ganas, 1997). Geomorphic expression of the fault extends to the east well beyond the Asprorema river and can be recognized for at least 3–4 km (Fig. 1C). To the west, the fault expression is well defined up to the Karagiozis river and continues for ca. 1.5 km toward Platirema river bounding a small plateau of Neogene and Quaternary deposits limited to the north by small but steep triangular facets.

It is interesting to notice that all along this fault section, the relatively small tectonic flexure on the alluvial fan deposits (generally 2–3 m high) controls the stream pattern. In fact, even though the major change in the erosional power of the streams along the fault trace occurs at the bedrock-alluvial fan boundary, erosion keeps incising the fan surface up to the flexure, which is the place of convergence of several stream sections that simulate the inception of brand new wine-glass valleys. Between Asprorema region and east of Atalanti, the mountain range shows a 300–310° strike with a gently concave trace. Just east of the town the mountain front forms a gentle promontory. West of this promontory the fault appears concave to the plain with a strike changing from 285° to 320°.

Moulkia Ruptures. Skouphos describes these ruptures as secondary to those along the Atalanti fault *sensu stricto*. He reports them as part of a 7-km-long lineament running, with a NE–SW trend, between the area known as Moulkia (a small village in 1894) and the major rupture at the southeastern tip of the Rhoda Mountains (Fig. 2). This rupture crossed the road between Atalanti and Proskinas with a radial set of fractures and produced an overall subsidence of 30–50 cm on the NW side of the Atalanti plain. No evidence for these ruptures was found during Lemeille's or our surveys. Conversely, Ganas (1997) and Ganas *et al.* (1998) interpret a fault plane exposed at site 25 as evidence for repeated activity on this transverse fault. This would be a link between the Proskinas–Kyparissi and Asprorema–Karagiozis rupture sections along the western slope of the Kourkouras–Kastri hills. We cannot rule out this possibility, however, we con-

Figure 7. (A) View from the north of the mountain range front, 100 m west of site 16 of Figure 3. Bedrock fault planes are visible on the slope along with huge fallen blocks (Mitsopoulos's flocks?). The 1894 scarp displaces *scree* and slope wash that blanket the lower part of the range front. Profile of Figure 8A was performed 100 m to the left. (B) Detail of the 1894 scarp (location in part A.), the field book on the left is near the crest of the scarp. Some modification for agricultural purposes occurred where the people are standing and may have affected the 1894 scarp-derived deposits.

sider the fault at site 25 to be minor with respect to the Atalanti fault. The western slope of the Kastri–Kourkouras hills does not show a substantial steepening at the base nor the expected high incision of the Agios Panteleimonas stream crossing the uplifted footwall (flowing from SSE to NNW, site 26 in Fig. 3), thus suggesting no important uplift. The Moulkia rupture in the alluvial plain does not show any evidence for long-term activity and presents a different strike relative to the Kourkouras hill slope. As a consequence, we suggest that the Moulkia rupture is (1) a lineament due to liquefaction features, (2) a surface effect of a buried contact between soft and hard sediments inherited from previous tectonic activity, or (3) due to buried artificial walls or levees built to control inundations in historic times (British Admiralty, 1847).

Moreover, the fault in the quarry and the alignment of the Asprorema river are violated at several places by Atalanti parallel faults. We suspect that the Asporema alignment/quarry fault is the northern portion of a preexisting complex crustal structure (herein after referred to as Rhoda structure) that substantially controlled the build up of the Chlomon mountains during rift and prerift tectonics. This appears today as the contact between the Triassic volcano-sedimentary unit of the Rhoda Mountains to the west and the Triassic–Jurassic dolomites and limestones to the east but does not have an obvious morphologic expression (Fig. 1C). On one hand, this main feature may be buried under the plain and show some sympathetic movement during the Atalanti fault activations. On the other hand, this structure may represent a strong geometric barrier controlling the Atalanti fault geometry instead of being an active part of a seismogenic source. As a consequence of this barrier a stepover in the main trace of the Atalanti fault forms between the Asprorema–Karagiozis and Proskinas–Kyparissi sections (Fig. 1C). Further support for this derives from the observation that long-term activity along the two proposed fault sections in the step over area would fully explain the observed geomorphology (see following discussion on this topic and Fig. 13).

The Western Part of the Mesoseismal Area in the Lokris (Renginion) Basin, from Atalanti to Ag. Kostantinos

The extent of the 1894 rupture west of Atalanti was also a matter of controversy among contemporary authors. Skouphos (1894) and Papavassiliou (1894a, b) claim that after having crossed the town of Atalanti, the rupture changed strike to a more NW direction, ran between the localities of Kalamaki and Arkouthari, cut the northeast slope of Epiknemis Mt. (part of the Knemis Mt.), and continued to the SW of Ag. Kostantinos dying out between this locality and Thronion (east of Kamena Vourla, see Fig. 1C). Conversely, Mitsopoulos (1894, 1895) states that the rupture ended at the Karagiozis valley, and no evidence for it existed between this valley and Ag. Kostantinos. Several other ground disruptions are described in this region by these authors, such

Table 3
1894 Earthquake Ruptures along the Western Section of the Atalanti Fault, Moulkia Structure, and Renginion Basin*

Site		Description
21 WAF	S	Atalanti town area: ruptures enclosing an elliptical region about 800 m long and 300 m wide with a 1- to 1.5-m change in elevation. Main rupture along the mountain slope and a secondary feature in the plain joining the main one near the *Pazari* spring (Pazari = market place; the building portrayed in Table 17).
	O	Not found.
	W	Main trace along the mountain slope and secondary antithetic splay are built on by houses and roads. At some places along the main fault, a change in steepness of the slope may be evidence for the 1894 scarp. Evidence for antithetic structure suggested by drainage pattern and topography. The *Pazari* spring no longer exists and could not be located precisely.
22 WAF	S	Ruptures along the northern slope of Rhoda Mt.
	O	Alluvial fan deposits displaced by the main fault. Lemeille (1977) and Rondoyinni (1984) tentatively attribute them to Riss age (190-130 Kyr).
	W	Left shore of the Asprorema river: 40- to 50-cm-high, N305°-striking fresh scarp well preserved for at least 200 m under a thick bramble over. Fresh scarp occurs at the base of 10- to 19-m-high escarpment in alluvial fan deposits (Figs. 8B and 12). Clear back tilt of fan surface in the hanging wall visible near the scarp; 30-cm-high secondary scarp located about 50 m away, experienced weather and human degrading.
23 WAF	S	Ruptures along the northern slope of Rhoda Mt.
	O	Not specifically mentioned.
	W	Scarp composed by three parallel branches in alluvial fan producing a cumulative displacement ranging between 2.7 and 3.5 m (Figs. 8C and 9). Interpreted as degraded cumulative scarps containing evidence for 1894 earthquake and previous ones. Hypothesis supported by trench excavations (Pantosti *et al.,* 2000).
24 WAF	S	Ruptures along the northern slope of Rhoda Mt.
	O	Not specifically mentioned.
	W	Wide flexure in alluvial fan deposits located some hundreds of meters off the main escarpment between Atalanti and Karagiozis river. Coseismic origin of this flexure confirmed through trenching (Pantosti *et al.,* 2000).
25 MR	S	7-km-long, NE–SW lineament between Moulkia (a small village in 1894) and major rupture at the southeastern tip of the Rhoda Mt. Lemeille (1977) and subsequently Rondoyianni (1984): the Moulkia rupture along the Asprorema river.
	O	Ganas (1997) and Ganas *et al.* (1998): fault plane in quarry in line with the position for the Moulkia rupture interpreted as evidence of its present activity.
	W	Quarry along the Asprorema river exposes a 220°-striking 80°W-dipping fault plane exhumed during the exploitation of alluvial terrace gravel; kinematic indications of oblique dextral movement. No evidence of active uplift in fault footwall.
27 RB	S	NW striking ruptures up to Ag. Kostantinos.
	O	Lemeille (1977): ruptures at the contact between limestone and Neogene deposits.
	W	Possible 1894 E–W striking rupture located at the base of Jurassic limestone slope encircled by Neogene soft deposits. Subsidence to the north. This setting does not suggest a primary tectonic origin, but rather a strong lithological control.
28 RB	S	NW-striking ruptures up to Ag. Kostantinos.
	O	Lemeille (1977) hypothesizes that the 1894 rupture may have utilized some Neogene fault planes that appear morphologically fresh.
	W	These fault planes crop out along the southern foothills of Profitis Elias Mt. with a WNW strike and subsidence to the south. Clear gravitational instability and intense erosion, secondary effects.

*Location of sites shown in Figure 3. WAF, West Atalanti Fault; MR, Moulkia lineament; RB, Renginon basin; S, from Skouphos (1894); O, from other works; W, this article.

as the impressive land movements that occurred near Megaplatanos village (old Skender-aga) that interrupted a stream flow producing a little lake (a site described in Lemeille [1977]), and the open fissures that seriously threatened the stability of the small village of Charma. Moreover, all along the coast, fractures and slumping occurred frequently with sand and water injection and blows that are typical evidence for liquefaction.

Skouphos' description of these ruptures does not contain many details of location, geometry, or size. However, Lemeille (1977) found possible evidence of them near Goulemi and near Kanapitsa (sites 27 and 28 in Table 3). No evidence for remnants of the ruptures indicated by Skouphos (1894) between Kalamaki and Arkouthari was found. These ruptures were probably located in the soft sediments of the northern slopes of the Knemis Mountains, used for agricultural purposes already at the time of Lemeille's survey.

From a geomorphic point of view the evidence of long-term activity of this part of the rupture is missing as already pointed out by Ganas (1997) and Ganas *et al.* (1998). No tectonic control on the drainage pattern or on the landform development suggestive for a continuation of the Atalanti fault in this area has been found, although secondary tectonic features exist even in Quaternary deposits (Kranis, 1999). A lineament with the same trend as the Atalanti fault is the 3.5-km-long, 290°-striking branch of the Alargino river (site 29, Fig. 3), whose valley is also quite well aligned with the possible evidence for 1894 ruptures at Goulemi. The mor-

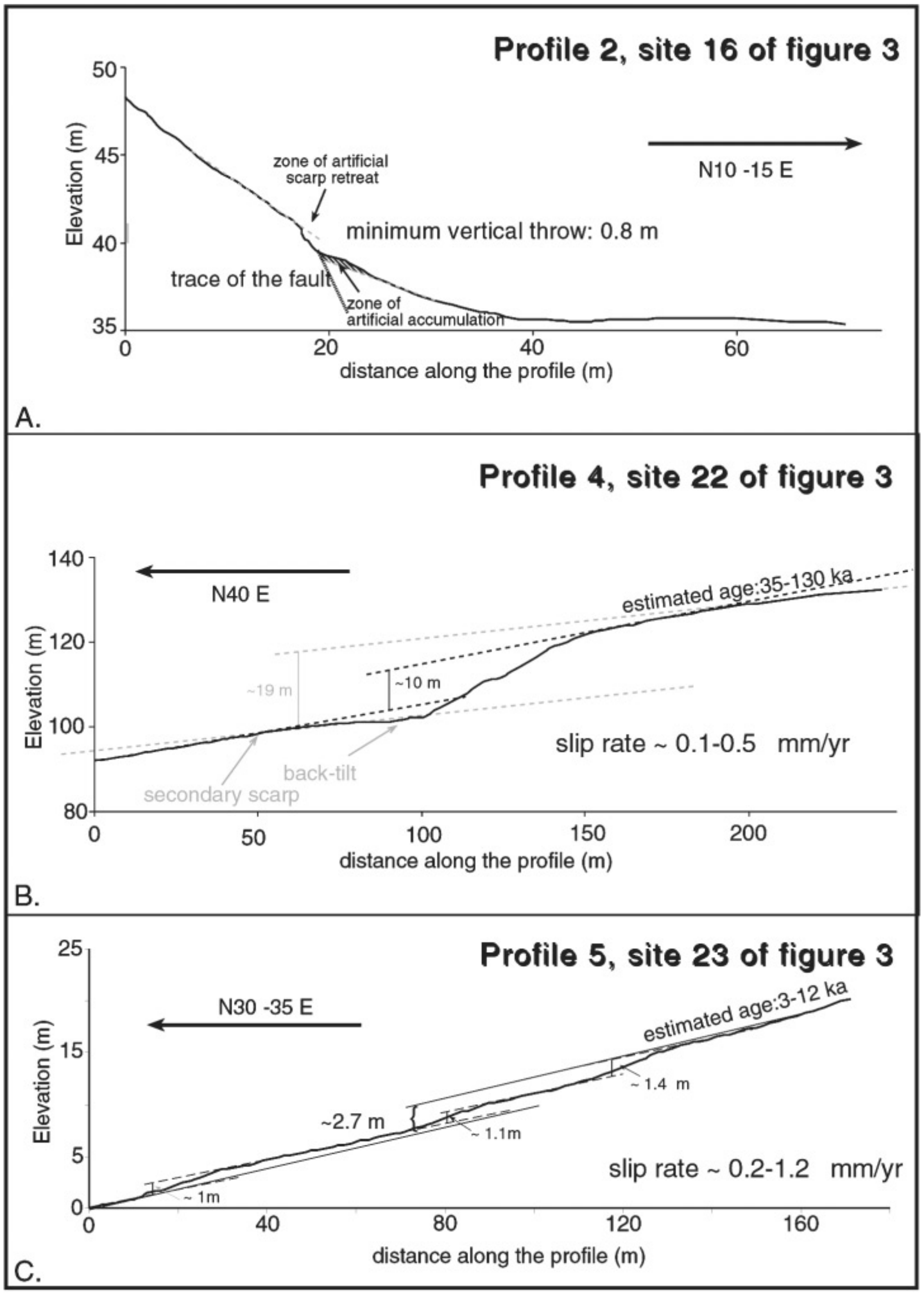

Figure 8. Detailed topographic profiles across the Atalanti fault at three sites. (A) Here some human modification occurred in the fault zone. The 1894 free face has been removed, and some spoils are left at the base of it (dashed zone). However, a rough estimate of the minimum vertical coseismic throw is still possible. (B) This profile cut across a cumulative fault scarp including the 1894 free face, displacing an abandoned alluvial surface. The scarp is highly degraded, but the human impact is still resolvable. The minimum and maximum total vertical displacements are estimated by assuming the original surface was parallel to that of the hanging wall far from the fault zone, or to that of the footwall far from the fault zone, respectively. Age of the displaced surface is not certain; see discussion it the text. (C) This profile intercepts three parallel cumulative scarps that highlight the possible complexity of the Atalanti fault expression at the surface. The total vertical throw produced by these three scarps in this abandoned alluvial surface has been estimated by summation of each individual scarp throw (3.5 m) or by assuming a planar displaced surface with no secondary depositional and erosional processes (2.7 m).

Figure 9. View from north of the three parallel scarps at site 23 of Figure 3. Notice that the three active scarps are well off the main range front. The arrows point at the crest of each of them. The net cumulative displacement produced by these features, measured through topographic profiling, ranges between 2.7 and 3.5 m. Recent trenching at this site has shown evidence for the 1894 ruptures and older events of surface faulting (Pantosti *et al.,* 2000).

phological evidence suggests that this valley is probably the result of erosion along a buried structure, with the same trend, that crops out in the hill south of Goulemi. This might imply that the Goulemi scarp is also related to older activity, and its limestone lithology has allowed for significant preservation of the landform. During the 1894 earthquakes, shaking may have caused gravitational sliding or differential compaction along old faults.

Moreover, the river valley, feeding the Loggos fan, appears completely undisturbed by a fault crossing through it as would be expected if the fault was continuing from Atalanti to Ag. Kostantinos. On the contrary, the river is cutting down into its valley, indicating it is controlled by the footwall uplift of the Arkitsa fault to the north instead of subsidence because of a long Atalanti fault. Finally, the possible evidence for 1894 ruptures appears completely incongruent with the statement of Skouphos (1894) that west of Atalanti the ruptures were following a more northwesterly trend toward Ag. Kostantinos. On the contrary, all the possible rupture sites found by Lemeille (1977), mapped also by Ambraseys and Jackson (1990) and during this work, are more westerly trending, clearly discontinuous, and also have opposite dip directions, probably mimicking previous structures or lithological contacts, a suggestion made also by Kranis (1999). This would suggest these are not primary tectonic ruptures but are due either to sympathetic slip on other active or buried structures or to strong shaking and gravitational effects.

Discussion: Main Open Questions on the 1894 Earthquake

The investigations performed on the Atalanti fault and on the 1894 earthquake leave open some important questions about the seismic behavior of the fault and the seismogenesis in the region. These questions concern the 1894 source location, extent, and geometry, the amount of slip and its variability along the fault, and the frequency of 1894-type events. In the following sections we discuss some of these topics.

Location of the 20 April Shock

It is well known that two shocks occurred a week apart on 20 April and 27 April, respectively. Even though all contemporary authors claim that the important ruptures occurred with the second and largest shock, the available information is not detailed enough to resolve the question of which are the faults responsible for them. Did they rupture two different portions of the Atalanti fault or two different faults? Similarly, are both events responsible for surface faulting? Assuming the first and smaller shock did not rupture the Atalanti fault, where did it occur? The Institute of Geology and Mineral Exploration (IGME) (1989) seismotectonic map of Greece reports the Atalanti fault as responsible for the 27 April shock only. Ganas *et al.* (1998) suggest that the 34-km-long fault they mapped through satellite imagery between Atalanti and Larymna may have ruptured during both events. It is clear that no discussion exists about the fact that the first event occurred somewhere to the east of the second one, offshore or inland in the vicinity of the Malessina peninsula. Some observations such as (1) the concentration of casualties due to the first shock in the villages of Proskynas, Malessina, and Martino (Mitsopoulos, 1894), (2) the occurrence of apparently tectonic ruptures during the first shock prevalently in Mazi and Malessina with a NE–SW direction, (3) the fact that Skouphos mentions the main rupture between Cape Gatza and Ag. Kostantinos only regarding the second shock, (4) the fact that the 40-km-long Atalanti fault is not sufficient to produce the two M_e 6.4 and 6.9 earthquakes, and (5) that there is no way to assume that the two earthquakes ruptured the same portion of the Atalanti fault a week apart allow us to propose a different hypothesis. It is possible that the Atalanti fault *sensu stricto* ruptured only during the second shock, at least between Larymna and Atalanti, and that the ENE–WSW Malessina structure may have ruptured during the first event (Fig. 11). Support for this hypothesis is derived also from C. Nostro (personal comm., 1999), that computing static stress changes using such a fault model, found that the location and geometry of the slip on the Malessina structure causes a significant increase in Coulomb stress on the NW section of the Atalanti fault. Increasing static stress may have favored fault interaction and could

Figure 10. View from the east of the western Atalanti range between Asprorema valley (to the left) and the town of Atalanti. Notice the large triangular facets and wine-glass valleys that characterize the range are typical of active normal fault mountain fronts.

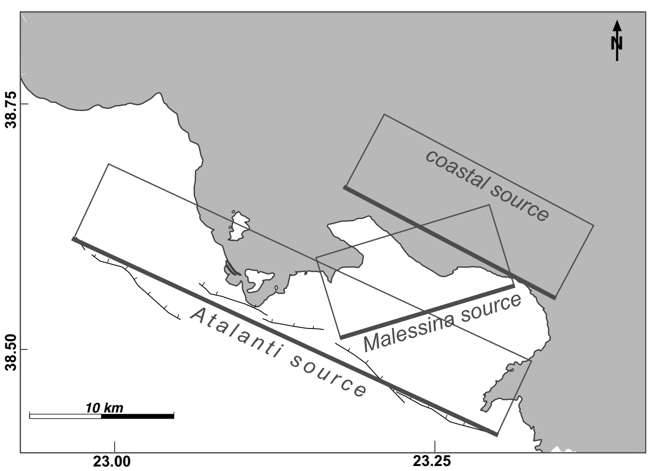

Figure 11. Possible sources for the 1894 shocks. Boxes are the surface projection of the sources assuming a 60°-dip of the fault and ~10-km-thick seismogenic layer. Thick lines are the surface fault plane intersections. The Atalanti source is responsible for the 27 April event. The source responsible for the 20 April shock is still ambiguous and could be either the Malessina or the coastal fault. Given its geometry, the Malessina fault would be a normal-oblique fault with a right lateral component. The coastal source is traced according to Ganas and Buck (1998).

explain the sequence of two shocks. Comparing the macroseismic estimates of magnitude for the first shock, which ranges between 6.4 and 6.7 (Ambraseys and Jackson, 1990; Makropoulos and Kouskouna, 1994; Papazachos and Papazachou, 1997), it appears that if we attribute to the Malessina structure an average coseismic slip of about 1 m, a length of 12 km, and a width of 12 km, we can reproduce M_e 6.4. No basis exists for extending the fault substantially offshore, or for increasing the coseismic slip to match M_e 6.7. The epicenter locations for the first shock of Ambraseys and Jackson (1990) and of Makropoulos and Kouskouna (1994) are consistent with the hypothesis of the activation of a 60° NW-dipping fault whose surface intersection coincide with the Malessina escarpment (Fig. 2).

However, the uncertainties on the location and geometry of the structure responsible for the first shock are important. There is no strong basis for ruling out other hypotheses, but at the moment we are not able to propose a better explanation. This is especially because on one side we are limited by the information that can be derived from contemporary descriptions of damage and effects because of proximity to the coast, the occurrence of two closely spaced shocks, and important secondary coseismic effects that increased the local damage. On the other hand, the geomorphic information is substantially limited because of submerged areas. At any rate, among the potential structures that ruptured during the first shock, we should consider an Atalanti-parallel offshore fault, north of the Malessina peninsula, as proposed by Ganas and Buck (1998) (Fig. 11), producing the uplift of the peninsula, which is strongly suggested by the existence of emerged marine terraces.

Length of the Fault Responsible for the 27 April Shock

Even at the time of the earthquake there was an intense discussion on the possible extent of the rupture to the northwest, up to Ag. Kostantinos. Mitsopoulos claimed that the main rupture was gravitational in nature following the contact between bedrock and alluvium and ended at the Karagiozis river, whereas, Skouphos and Papavasiliou said the rupture extended much further to the NW. Skouphos reports discontinuous ruptures between Atalanti and Ag. Kostantinos but describes them very superficially, suggesting they were substantially less important than those between Tragana and Atalanti. Even if discontinuous, these ruptures coupled with the important damage produced in the coastal area near Ag. Kostantinos were successively considered by several authors as the result of a longer structure extending as far as Ag. Kostantinos. The fact that the fault may extend below the Lokris (Renginion) basin between Atalanti and Ag. Kostantinos has a very strong impact on hazard calculations, making the Atalanti seismic source fault 20 km longer. As pointed out already by Ganas *et al.* (1998) the overall geomorphology of this area is not suggestive of any major structure on the continuation of the Atalanti fault with exception of a few-km-long lineaments close to the Atalanti plain. Moreover, Collier and Gawthorpe (1994) by using drainage patterns define quite convincingly the NW boundary of the Atalanti fault. In fact, they locate north of the Karagiozis river a major transfer zone between the Atalanti fault and the Arkitsa fault. This transfer zone is interpreted as a zone where topographic differentials develop along border-fault footwalls because the slip on both faults decreases to zero toward fault ends. This allows a major drainage convergence and the development of catchments much wider than those typical of the fault footwall. If this model is correct, the eastern Lokris basin would represent a transfer zone, and it contains no evidence for typical footwall uplift. Most of the locations, where Skouphos described ruptures in the Renginion Basin, appear as high instability or lithological contact areas. Here shaking may be the principal cause for their formation. Given all of this, it seems conceivable to consider the ca. 32-km-long Atalanti fault, between Larymna and Karagiozis river, as the source responsible for the 27 April shock. It is clear that the damage distribution propounds for a longer fault, up to 60 km. However, the important damage in Ag. Kostantinos can be a combined effect of (1) possible NW directivity of rupture propagation, (2) physical and geotechnical properties of sediments favoring liquefaction and landsliding, (3) overlap of damage from both events (Albini, 2000).

The extent of the rupture to the southeast is unclear too. In this case the difference between the rupture extent indicated by Skouphos, up to Cape Gatza, and what we were able to recognize, only up to Larymna, is about 8 km. As already discussed, because of preexisting fabrics in the upper crust to the east of Larymna, the rupture may have divided on different splays and lost its typical geomorphic expression.

Thus, the total extent of the 27 April rupture ranges from a minimum of 32 km (Karagiozis-Larymna) to a maximum of 58 km (Cape Gatza–Ag. Kostantinos) with the smaller figure preferred.

Fault Behavior

In the following section, we discuss coseismic slip, slip rate, and recurrence time. These are the major parameters, along with fault length, that define the seismic fault behavior for hazard purposes.

Coseismic Slip. The only direct measures of the 1894 coseismic slip are derived from the contemporary descriptions of Skouphos (1894). In general, vertical throws he observed were close to 1 m with a 2-m maximum in soft rocks and a 30-cm minimum in hard limestone. Openings were up to 1.5 m with 5 cm to 4 m ranges. It is not clear how these measurements were taken. The openings appear particularly suspicious and suggestive of local major superficial sliding. Unfortunately, no contemporary detailed maps have been published to help in better understanding the coseismic slip distribution. As already mentioned, Ganas *et al.* (1998) measured a notch in a freshwater spring 53 cm higher than the present water level, and our observations on scarps in bedrock and colluvial deposits suggest a minimum displacement between 30 and 80 cm (see sites in Table 2). These values are essentially validated by recent trench excavations (Pantosti *et al.,* 2000).

On the basis of (1) our field survey, (2) photographs taken in the 1970s by Lemeille, and (3) the geometry of the structures encountered in the trenches, it seems that the rupture was composed by parallel splays, both synthetic and antithetic (Figs. 6 and 9). At some locations these splays were concentrated within a few meters, whereas in others they may reach the surface a few hundreds of meters away (i.e., one at the contact bedrock scree, another or more in the colluvium or alluvium). The ruptures that occur in close parallel or subparallel strands are very common in normal faults. In general, geologists are attracted by faults in the bedrock and this definitely occurred along the Atalanti fault in the past, but this meant looking at only one part of the coseismic deformation. In fact, it is well known from the international literature that in prevalently normal faults (e.g., Wallace, 1984; Crone *et al.,* 1987; Zhang *et al.,* 1990), the main coseismic ruptures frequently form not exactly where the bedrock fault is outcropping but toward the basin, in soft recent sediments. This is probably an effect of the rupture propagation when the thickness of soft sediments overlaying the bedrock reaches a critical value. This may also explain the highest throws in the alluvial sediments rather than in the bedrock reported by Skouphos (1894), a difference that was generally attributed to local compaction or gravitational effects instead (Figs. 6 and 9). Therefore, measurements of coseismic slip on individual fault splays may underestimate the true slip at the surface produced by the 1894 earthquake.

By using the empirical relations proposed by Wells and Coppersmith (1994) to compare total length of the surface rupture with the average displacement for normal faults, it appears that for a 32-km-long rupture, which is our preferred figure (see previous discussion), a ∼1-m displacement is expected. This is totally in agreement with the Skouphos observations.

From Skouphos' report (1894) there is also evidence for horizontal movement. This is described as a movement of the hanging wall toward the NW, which would suggest a left lateral component as already highlighted by Richter (1958) and IGME (1989). However, there is not enough information to quantify this component. It is only clear that it is minor with respect to the vertical, as expected also from the long-term geomorphology. This information is given also without referring to specific localities, a fact preventing us from understanding if this is only a local effect due to the fault geometry or is diffused all along the fault extent.

Slip rate. The only estimate of slip rate available for the whole fault is that proposed by Ganas (1997) and Ganas *et al.* (1998). Assuming they could locate sites that were all lying at the same horizontal surface before being faulted, they compare 14 pairs of measurements across the fault between Karagiozis and Mt. Skorponeri (see Figs 6 and 7 in Ganas *et al.,* 1998). From their data, fault throws reach zero at the fault boundaries, thus supporting the hypothesis of a fault not extending further to the NW, and highest throws are obtained in the Asprorema area both for prerift and for synrift deposits: 1200 and 810 m, respectively. Constraints for the age of the inception of the faulting are not available. Adopting an age of 3 Ma, Ganas *et al.* (1998) calculated a maximum slip rate for this fault varying between 0.27 and 0.4 mm/yr. It is clear that this estimate is very questionable because it is based on too many assumptions and little direct observation; however, it is the first proposed slip rate for this fault.

We attempted evaluations of slip rates for Late Pleistocene, however, the lack of clearly displaced Late Pleistocene datums and absolute dating prevented us from obtaining strongly reliable values. As a consequence, we have only one conceivable evaluation of Late Pleistocene slip rate in the Asprorema area (site 22 in Fig. 3). Here an alluvial fan surface is displaced by the fault 10 to 19 m (Figs. 8B and 12). There is no absolute dating of this fan. Rondoyianni (1984) attributed it to Riss age (190–130 kyr). Being in a coastal plain environment and being part of the penultimate alluvial fan generation in the area, we would expect this fan to be deposited mainly during the warm period postdating the Riss glacial, and thus between 130 and 35 kyr (see Chappell [1983] for reference). If we are correct, this would yield a slip rate in the range 0.1–0.5 mm/yr in apparent agreement with Ganas *et al.* (1998).

Figure 12. View from north of the Asprorema valley close to site 22 of Figure 3. The abandoned alluvial surface with olive trees, clearly visible on the right of the valley, is displaced 10 to 19 m (see Fig. 8B) along a major escarpment by repeated movement on this strand of the Atalanti fault. Important fault traces are exposed in the river banks below the main escarpment and show prevalent normal movement. In the background one of the highest peaks of the Chlomon range (∼1100 m).

Finally, we attempted an estimate of the Holocene slip rate at a location east of Atalanti (site 23 in Fig. 3) where the fault splays in three parallel branches and displaces Holocene alluvial fan deposits and cultural layers by 2.7–3.5 m (Figs. 8C and 9). We estimate 12 kyr as maximum age for the faulted deposits and 3 kyr as minimum (based on correlation with classical period characterized by large diffusion of pottery). This would yield a Holocene slip rate of 0.2–1.2 mm/yr.

Earthquake Recurrence. What is the age of the penultimate event on the Atalanti fault? The answer to this question has a very strong impact on the seismic potential associated with this fault. Whether it commonly produces one $M \sim 7$ event per century or per millennium makes a big difference. In 426 B.C., at least two large earthquakes struck the broader region, as we know from ancient writers (Thucydides, who was living at the time of the earthquake, Diodore the Sicilian, and Strabo, see Bousquet and Pechoux [1977]). The second earthquake caused significant damage in the Atalanti area (ancient Opous), producing also a tsunami wave that flooded the Atalanti plain. Diodore reported subsidence of the coast, that caused the formation of the present-day Atalanti island, something which has been disputed by Fossey (1990) who believes it is a mistake of Diodoros whose writings contradict writings by Thucydides that clearly state Atalanti was an island 5 years before the earthquake. Bousquet and Pechoux (1977), Makropoulos and Kouskouna (1994), and Papazachos and Papazachou (1997) rule out the possibility that the 426 B.C. event may have occurred on the Atalanti fault and claim that even if limited in details, the damage reports would call for an event located much to the northwest, in the Maliakos Gulf. On the contrary, Ganas (1997) and Ganas *et al.* (1998) suggest that the 426 B.C. earthquake may have occurred on the Atalanti fault because their geological evaluations of slip rates and slip per event yield a very crude average recurrence time of 2500 yr. This evaluation may be totally correct, however, it does not at all imply that the 426 B.C. event occurred on this fault. According to Stiros (1988) and Stiros and Pirazzoli (1995) the *stoa* located on or close to the Atalanti fault trace (site 19 in Fig. 3) was suddenly abandoned in 450 B.C., probably because of the collapse due to an earthquake. Assuming that the 426 B.C. earthquake ruptured the Atalanti fault, they conclude that large earthquakes on this fault may be separated by a period as short as only 25 years. This appears unlikely and poorly supported by datings. The age of the event that occurred prior to the 1894 event remains an open question.

Finally, in terms of earthquake recurrence, it is worth mentioning the excellent intuition that Skouphos had about earthquake location, repetition, and growth of geological structures. In his report (1894) he writes that, considering that the Holy Friday earthquake (27 April) produced in Atalanti about 2 m of subsidence, if this earthquake would repeat with similar characteristics every year, in a period of 90 years, the town, now about 180 m above sea level would be submerged. Thus, about at the same time Gilbert (1884) had a similar intuition because of the Owens valley earthquake in the western United States, the "strenuous young scientist" Skouphos (as he was called—ironically—by Mitsopoulos, professor at that time) was able to propose a first understanding of the repetitive characteristics in terms of time and space of large earthquakes and of their control on the evolution of the landscape in seismic areas.

Control of Transversal Structures on the Geometry of the Atalanti Fault

The presence of preexisting texture in the crust surely produces a control in the geometry of faults and coseismic slip distribution (see, for example, Pantosti and Valensise [1990] and Valensise and Pantosti [2001]). This is also the case with the Atalanti fault that, as already discussed, is clearly controlled by structures such as Rhoda, Malessina, Pavlos, and NW Chlomon (Figs. 1C, 3, and 11) and the probable Vivos Fault (according to Ganas *et al.,* 1998). Geomorphology indicates that the rates of activity of these structures are very low or they are inactive. The Malessina and Vivos faults produce a gentle bend in the Atalanti fault trace and, at the same time, a scattering of the deformation that causes difficulty discerning the long-term evidence of the fault. The Pavlos fault seems to play the role of a geometric barrier for the Atalanti fault propagation toward the SE. In fact, after the two faults intersect south of Larymna, no obvious evidence for the Atalanti fault trace has been found either in the air photos or in the field. Whether the fault dies out at this intersection or the deformation is diffused over a wider volume of crust is not obvious. In a similar way to the Pavlos fault, the old fault zone that bounds Chlomon Mountain to the NW (which is also the boundary between Alpine and Neogene formations and is followed by Karagiozis river at its exit out of Rhoda mountains) limits the fault propagation towards the NW. Across the Rhoda structure, the Atalanti fault makes a 5-km-wide left-lateral stepover. Poulimenos and Doutsos (1996) interpret this complexity as an asperity that developed into a nonconservative barrier that, with time, developed several N75° and N130°-oriented fault segments, that produced a net of faults east of the stepover. The western slope of the Kourkouras–Kastri hills is mapped as one of these N75° segments and is considered responsible for more than 1000 m subsidence of the plain.

Ganas *et al.* (1998) claim that now, the Atalanti fault is linked through the stepover that existed only when the Atalanti fault was formed by two protosegments. In fact, the Asprorema-exhumed fault plane, which bounds the Kourkouras–Kastri hills to the west, and the abrupt lithological contrast shown by some electric profiles are considered evidence for a continuous Atalanti Fault between Kiparissi and Atalanti. As already discussed, the Kourkouras–Kastri hills footwall does not show geomorphic evidence of uplift controlled by such a fault transversal to the Atalanti structure. The contact between limestones and synrift deposits (Neogene) interpreted from electrical data may be the long-term result of prerift and synrift tectonics coupled with recent slip on the Proskinas–Kyparissi section. Moreover, by modeling the expected elevation changes produced by the faults (Karagiozis–Asprorema and Kiparissi–Proskinas) forming the stepover (Fig. 13A), the present geomorphology appears totally consistent with a left stepover without calling for a more complicated interpretation. In the stepover, the uplift of the footwall of the Kiparissi–Proskinas section is balanced by the subsidence induced by the Asprorema–Karagiozis section. This produces an interesting area of essentially no vertical changes enclosed between the two uplifted footwalls of the Kiparissi–Proskinas, to the east, and Karagiozis–Asprorema fault, to the west. This area forms a corridor in a NNW direction that represents a favorable situation for the active stream crossing the Kourkouras–Kastri hills (Ag. Panteleimonas stream) to flow (site 26 in Fig. 3). Moreover, the Kourkouras–Kastri hills are not part of a typical uplifting footwall but participate in the general subsidence of the plain even though with minor values. This could explain both the gentle morphology of the hills and the lack of obvious incision of the Ag. Panteleimonas stream. At this purpose it is interesting to notice the different morphology associated with the active stream crossing the Kourkouras–Kastri hills and the Mesophorou stream (site 30 in Fig. 3) obviously cutting through the uplifting Kiparissi–Proskinas footwall. Modeling of the elevation changes considering a fault with a sharp bending around the Kourkouras hill (Fig. 13B) clearly shows that an important subsidence is expected west of these hills in contrast to their uplift. Although the differences between the two models are not sufficient to prefer one of them, the situation in Figure 13B seems not to completely fit the present geomorphology.

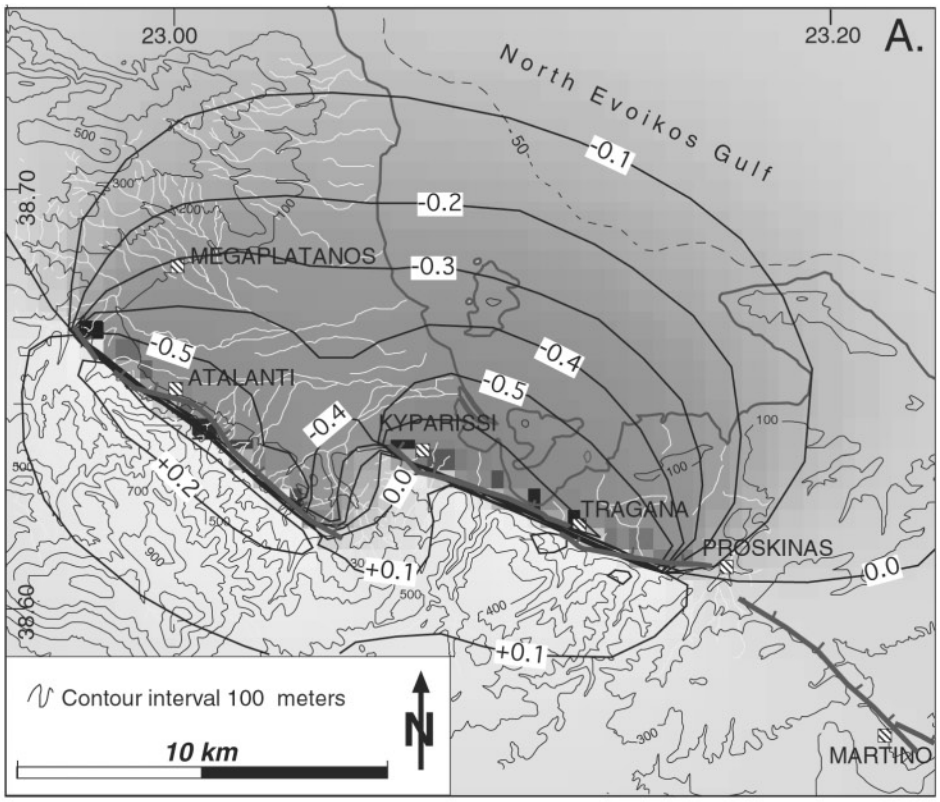

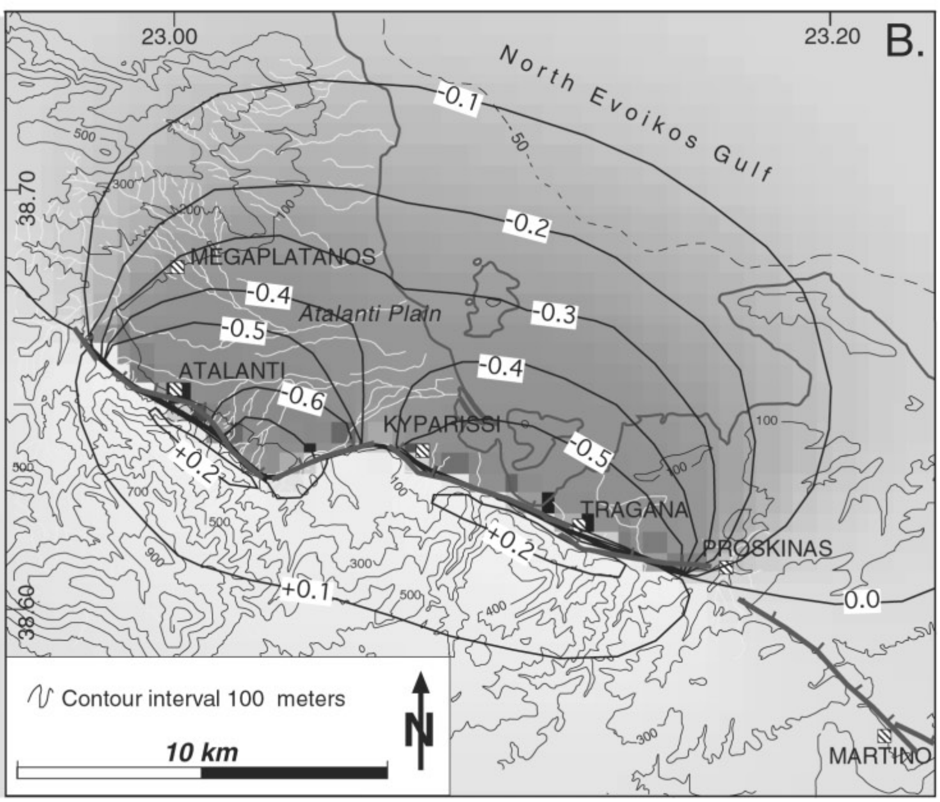

Figure 13. Dislocation models across the Asprorema stepover assuming different geometry of faults. The expected displacements were modeled as the response to simple dislocation along planar rectangular faults embedded in an elastic half-space. The calculations were performed with a code developed by Ward and Valensise (1989) based on standard dislocation theory. Subsiding and uplifting areas are shown in dark and light gray, respectively. For all the faults we assumed standard normal fault parameters (dip 60°, rake 270°) and unitary slip. In Figure 13A, the faults are separated by a 3-km-wide left stepover, whereas in Figure 13B the fault forms a sharp bend and bounds at the base the Kourkouras–Kastri hills. This produces an important uplift of these hills opposite to the amphitheater-shaped subsidence resulting from the fault setting in Figure 13A. The gentle geomorphology and the lack of strong incision shown by the Panteleimonas stream (site 26 in Fig. 3) crossing the hills suggest that no important uplift occurs. Note that the Atalanti plain and the gulf in front of it are nicely enclosed in the subsiding area as predicted in both models.

To summarize, from our observations the existence of a linkage between the Proskinas–Kiparissi and Asprorema–Karagiozis fault sections along the western slope of the Kourkouras–Kastri hills is not obvious but cannot be ruled out. Conversely, according to the Skouphos (1894) report, it seems that a possible linking occurred to the east of the Kourkouras–Kastri hills, between Kiparissi and Ag. Panteleimonas (site 20 in Fig. 3). The Moulkia rupture appears totally disconnected from the main fault.

Conclusions

On the basis of aerial photo and field survey, we remapped the remnants of the 1894 earthquake ruptures along with the evidence for long term activity of the Atalanti fault. Despite the intense human modification due to bulldozing for agricultural purposes, and substantially guided by Lemeille's (1977) survey that predated this modification, we have been able to locate the 1894 rupture at several sites and reconstruct the overall geometry of the fault. We tried to document with as much detail as possible the 1894 ruptures to provide a reliable reference both for future paleoseismological studies and for seismic potential assessment of nearby faults. Several observations indicate that preexisting structures control the geometry of the Atalanti fault, producing gentle bends and scattering of the deformation where the Atalanti fault intercepts their trace. The Rhoda structure in particular seems to play the role of a geometric barrier that caused a left stepover in the Atalanti fault (Fig. 1C).

Remnants of the 1894 ruptures are found along the fault over a distance of ca. 32 km between Larymna and the Karagiozis river. In a few cases it is possible to observe degraded 30 to 50 cm high free-faces both in limestone and in slope deposits. In most of the cases the 1894 ruptures are part of cumulative scarps in alluvial and colluvial deposits, now degraded and retreated by intense agricultural activity. Complexity of the rupture, generally including multiple splays, can be observed in the geomorphology and has been confirmed by recent trench excavation. The average vertical throw measured by Skouphos (1894) is 1 m; the throws that we could still measure are up to 0.8 m. However, this latter figure should be considered a minimum both because our measurements are in general minimums because of the time elapsed since their formation and the existence of multiple splays. Although written and field evidence is inadequate to definitely conclude which are the sources of the first and the second shocks, we suggest that the Atalanti fault *sensu stricto* ruptured only during the second shock (27 April) and that the first shock (20 April) may have occurred either on the Malessina fault or offshore on a Atalanti parallel fault. The 27 April ruptures extend at least between Larymna and Karagiozis river for about 32 km; however, both Skouphos' report and Ganas *et al.* (1998) satellite analysis suggest the fault could extend ca. 8 km further, up to Cape Gatza. No convincing evidence for a further extent of the fault rupture has been found between the Karagiozis river and the town of Ag. Kostantinos. We conclude that all the ruptures observed in the area have a gravitational, differential compaction, or liquefaction origin.

By using the empirical relations proposed by Wells and Coppersmith (1994) both for magnitude vs. rupture length, and average displacement vs. rupture length, there is an agreement between the M 6.9 for the 27 April event (Ambraseys and Jackson, 1990), a surface rupture length of 32–40 km, and a 1 m average vertical throw at the surface. Similarly, the moment associated with a 32 to 40 km long, 12 km wide fault with 1.5 m slip at depth (assuming that at the surface we observe only a 60% of the slip on the fault at depth, see for example as in Pantosti and Valensise [1990], Wells and Coppersmith [1994]), ranges between 1.73×10^{26} and 2.16×10^{26} dyne/cm, that translate to a ca. 6.8 magnitude.

Slip rates and recurrence intervals are still poorly constrained for this fault. However, according to both Ganas *et al.* (1998) and this work, the most common figure of slip rate ranges between 0.1 and 0.5 mm/yr, with a possible 1 mm/yr maximum in the Holocene. These values indicate that in this area crustal extension rates are much slower than in nearby seismic regions such as the Gulf of Corinth. Recurrence intervals appear to be on the order of millennia, however, we rule out the possibility that the 426 B.C. ruptured this fault.

Acknowledgments

We are grateful to G. Valensise for his encouragement and for providing the dislocation program used to obtain Figure 13, to Guglielmo and Alberto Frepoli for translating the Skouphos article, to H. Maroukian, P. Gaki-Papanastassiou, and G. D'Addezio for their support and discussion in the field, and to B. Angioni for providing graphic support. We are also indebted to the mayor of the town of Atalanti and to the staff of the local Archaeological Office and in particular to Mrs. F. Dakoronia and S. Dimaki for their precious cooperation. The manuscript benefited from throughout reviews from N. N. Ambraseys, S. Pavlides, and L. Grant. The European Community project FAUST (ENV4-CT97-0528) funded most of this work with additional funding of Istituto Nazionale di Geofisica e Vulcanologia and National Observatory of Athens.

References

Albini, P. (2000). Una rilettura dei forti terremoti del 20 e 27 Aprile 1894 nella Locride (Grecia centrale), G.N.G.T.S. XIX National Congress, extended Abstracts volume, 190–191, C.N.R., 7–9 Nov., Roma (in Italian).

Ambraseys, N. N., and J. A. Jackson (1990). Seismicity and associated strain of central Greece between 1890 and 1988. *Geophys. J. Int.* **101,** no. 3, 663–708.

Armijo, R., B. Mayer, G. C. P. King, A. Rigo, and D. Papanastassiou (1996). Quaternary evolution of the Corinth Rift and its implications for the late Cenozoic evolution of the Aegean, *Geophys. J. Int.* **126,** 11–53.

Bousquet, B., and P.-Y. Pechoux (1977). La sismicité du Bassin Egeen pendant l'antiquité. Méthodologie et premiers resultats, *Bull. Soc. Geol. France* **19,** no. 3, 679–684.

British Admirality (1847). Gulf of Volos with Oreos and Atalanti channels, British Admirality Map 1556, scale 1:100.000, Survey of 1846–1847.

Chappell, J. M. (1983). A revised sea-level record for the last 300,000 years from Papua New Guinea, *Search* **14,** 99–101.

Collier, R. E. Ll., and R. L. Gawthorpe (1994). Neotectonics, drainage and sedimentation in central Greece: insights into coastal reservoir geometries in synrift sequences, *Hydrocarbon Habitat in Rift Basins,* J. J. Lambiase (Editor), Geol. Soc. Spec. Publ. 80, 165–181.

Crone, A. J., M. N. Machette, M. G. Bonilla, J. J. Lienkaemper, K. L. Pierce, W. E. Scott, and R. C. Bucknam (1987). Surface faulting accompanying the Borah Peak earthquake and segmentation of the Lost River fault, central Idaho, *Bull. Seism. Soc. Am.* **77,** 739–770.

Cundy, A. B., S. Kortekaas, T. Dewez, I. S. Stewart, I. W. Croudace, H. Maroukian, D. Papanastassiou, P. Gaki-Papanastassiou, K. Pavlopoulos, and A. Dawson (2000). Coastal impacts of the 1894 Gulf of Atalanti earthquakes, central Greece, *Marine Geology Spec. Publ.* **170,** 3–26.

Davison, C. (1894). M. Papavasiliore on the Greek earthquakes of April 1894, *Nature* **1303,** no. 50, 607.

Fossey, J. M. (1990). The Ancient Topography of Opuntian Lokris, J. C. Gieben, Amsterdam.

Ganas, A. (1997). Fault segmentation and seismic hazard assessment in the gulf of Evia rift, Central Greece, *Ph.D. Thesis,* University of Reading, U.K., 368 pp.

Ganas, A., and V. A. Buck (1998). A model for the tectonic subsidence of the Allai archaeological site, Lokris, central Greece. *Bull. Geol. Soc. Greece* **32,** no. 1, 181–187.

Ganas, A., and White, K. (1996). Neotectonic fault segments and footwall geomorphology in eastern Central Greece from Landsat TM data, Geol. Soc. Greece Spec. Publ. 6, 169–175.

Ganas, A., G. P. Roberts, and T. Memou (1998). Segment boundaries, the 1894 ruptures and strain patterns along the Atalanti fault, Central Greece, *J. Geodynamics* **26,** no. 2–4, 461–486.

Gilbert, G. K. (1884). A Theory of earthquakes of the Great Basin, with practical application, *Am. J. Sci.* **3,** no. 27, 49–53.

Institute of Geology and Mineral Exploration (IGME) (1989). Seismotectonic map of Greece, IGME, Athens, scale 1:500,000.

Karnik, V. (1971). *Seismicity of the European Area,* Reidel Publishing Co., Dordrecht, Holland, pp. 218.

Kranis, H., (1999). Neotectonic activity of fault zones in Central-eastern Sterea Hellas (Lokris), *Ph.D.* Thesis, University of Athens, 233 pp. (in Greek).

Lemeille, F. (1977). Etudes néotectoniques en Grèce centrale nord-orientale (Eubée centrale, Attique, Béotie, Locride) et dans les Sporades du Nord (île de Skiros), Thèse de Troisieme Cycle Université Paris XI—Centre Orsay, 173 pp. (in French).

Ma, X. Q., and N. J. Kusznir (1995). Coseismic and postseismic subsurface displacements and strains for a dip-slip normal fault in a three-layer elastic-gravitational medium, *J. Geophys. Res.* **100,** 12,813–12,828.

Makropoulos, K. C., and V. Kouskouna (1994). The 1894 April 20 and 27 Atalanti Earthquakes: 100 years after. Lessons learnt, in *Proc. and Activity Report of the 1992-94 XXIV European Seismological Commission,* Athens, Greece, September 1994, Vol. 1, 61–71.

Mitsopoulos, K. (1894). Die Erdbeben von Theben und Lokris in der Jahren 1893 und 1894, *Abdruck aus Dr. A. Petermanns Geogr. Mitteilungen* **10,** 1–11 (in German).

Mitsopoulos, K. (1895). *The Mega-earthquake of Lokris in April 1894,* Ethnikon Typografeion, Athens, 40 pp. (in Greek).

Pantosti, D., and G. Valensise (1990). Faulting mechanism and complexity of the 23 November 1980, Campania-Lucania earthquake, inferred from surface observations, *J. Geophys. Res.* **95,** 15,319–15,341.

Pantosti, D., P. M. De Martini, D. Papanastassiou, N. Palyvos, F. Lemeille, G. D'Addezio, L. McNeill, K. Gaki-Papanastassiou, and G. Stavrakakis, (2000). Geomorphological and Paleoseismological studies of the Atalanti fault (central Greece), ESC XXVII General Assembly, Book of Abstracts, 10–15 September 2000, Lisbon, Vol. 73.

Papavassiliou, A. (1894a). Sur le tremblement de terre de Locride (Grèce) du mois d' Avril 1894, *C. R. Acad. Sci. Paris* **19,** 112–114 (in French).

Papavassiliou, A. (1894b). Sur la nature de la grande crevasse produite à la suite du dernier tremblement de terre de Locride, *C. R. Acad. Sci. Paris* **19,** 380–381 (in French).

Papazachos, B. C., and C. B. Papazachou (1997). *The Earthquakes of Greece,* P. Ziti & Co., Thessaloniki, 304 pp.

Philip, H. (1974). Etude néotectonique des rivages Égéens en Locride et en Eubée north-occidentale (Grèce), *Thèse de Troisième Cycle,* Ac. de Montpellier, Univ. Sc. Techn. du Languedoc, 103 pp. (in French).

Philippson, A. (1894). Das dies jahrige Erdeben in Lokris, *Zeitschrift Ges. Erdkunde zu Berlin* **21,** 332–334 (in German).

Poulimenos, G., and T. Doutsos (1996). Barriers on seismogenic faults in central Greece, *J. Geodynamics* **22,** 119–135.

Richter, C. F. (1958). *Elementary Seismology,* Freeman, San Francisco, 768 pp.

Roberts, S., and J. Jackson (1991). Active normal faulting in central Greece: an overview, in *The Geometry of Normal Faults,* A. M. Roberts, G. Yielding, and B. Freeman (Editors), Geol. Soc. Sp. Publ. 56, 125–142.

Rondoyianni, T. (1984). Etude néotectonique des rivages occidentaux du canal d'Atalanti (Grèce Centrale), *Thèse de Troisième Cycle,* Université Paris-Sud-Centre d'Orsay, 193 pp. (in French).

Skouphos, T. (1894). Die swei grossen Erdbeben in Lokris am 8/20 und 15/27 April 1894, *Zeitschrift Ges. Erdkunde zu Berlin* **24,** 409–474 (in German).

Stiros, S. (1988). Archaeology: a tool to study active tectonics. The Aegean as a case study, *EOS* Trans. Am. Geophys. Union, **69,** no. 50, 1633–1639.

Stiros, S. C., and T. Rondoyianni (1984). Recent vertical movements across the Atalanti fault-zone (central Greece), *Pageoph.* **123,** 837–848.

Stiros, S. C., and P. A. Pirazzoli. (1995). Palaeoseismic studies in Greece: a review, *Quaternary International* **25,** 57–63.

Valensise, G., and D. Pantosti (2001). The investigation of potential earthquake sources in peninsular Italy: a review, *J. Seismology* (in press).

Wallace, R. E. (1984). Fault scarps formed during the earthquakes of October 2, 1915, in Pleasant valley, Nevada, and some tectonic implications, *U. S. Geol. Surv. Prof. Pap. 1274-A,* 33 pp.

Ward, S. N., and G. Valensise (1989). Fault parameters and slip distribution of the 1915, Avezzano, Italy earthquake derived from geodetic observations, *Bull. Seism. Soc. Am.* **79,** 690–710.

Wells, D. L., and K. J. Coppersmith (1994). New empirical relationships among magnitude, rupture length, rupture width, rupture area, and surface displacement, *Bull. Seism. Soc. Am.* **84,** 974–1002.

Zhang, P., M. Ellis, D. B. Slemmons, and F. Mao (1990). Right-lateral displacements and the Holocene slip rate associated with prehistoric earthquakes along the southern Panamint Valley fault zone: implication for southern basin and range tectonics and coastal California deformation, *J. Geophys. Res.* **95,** 4857–4872.

Instituto Nazionale di Geofisica e Vulcanologia
Via di Vigna Murata 605
I-00143 Roma, Italy
(D. Pantosti, P.M.D.)

National Observatory
Athens, Institute of Geodynamics
P.O. Box 20048 Gr-11810, Greece
(D. Papanastassiou, G.S.)

University of Athens, Department of Geology
Panepistimiopolis Zografou, 157 84
Athens, Greece
(N.P.)

Institut de Protection et de Sûreté Nucleaire
F-92265 Fontenay-Aux-Roses
Cedex, France
(F.L.)

Manuscript received 31 March 2000.